Biosensors and Bioelectronics 64 (2015) 219–226

Contents lists available at ScienceDirect

Biosensors and Bioelectronics

journal homepage: www.elsevier.com/locate/bios

Selective protein detection with a dsLNA-functionalized nanopore

Paola Fanzio [a,*], Valentina Mussi [b], Michele Menotta [c], Giuseppe Firpo [a], Luca Repetto [a], Patrizia Guida [a], Elena Angeli [a], Mauro Magnani [c], Ugo Valbusa [a]

[a] Department of Physics, University of Genoa, via Dodecaneso 33, 16146 Genova, Italy
[b] National Research Council, Institute for Complex Systems ISC-CNR, Via del Fosso del Cavaliere 100, 00133 Roma, Italy
[c] Department of Biomolecular Sciences, University of Urbino 'Carlo Bo', Via Saffi 2, 61029 Urbino, PU, Italy

ARTICLE INFO

Article history:
Received 14 July 2014
Received in revised form
10 August 2014
Accepted 27 August 2014
Available online 6 September 2014

Keywords:
Biosensor
Nanopore
Protein detection
NF-κB
Functionalization

ABSTRACT

In the last years, nanopore technology has been increasingly exploited for biomolecule detection and analysis. Recently, the main focus of the research has moved from the study of nucleic acids to the analysis of proteins and DNA-protein complexes. In this paper, chemically functionalized solid-state nanopore has been used to recognize Nuclear Factor-kappa B proteins (NF-κB), that are involved in several disorders and inflammation processes, so that their identification is of crucial importance for prognostic applications. In particular, we show that it is possible to electrically detect the specific interaction between p50, a protein belonging to the NF-κB family, and dsLNA probe molecules covalently attached to the surface of a FIB fabricated SiN pore. The obtained results have been compared with those related to BSA protein, which does not interact with the used probes. Finally, the potential of the device has been further tested by analyzing a whole cell extract. In this case, three principal peaks in the distribution of electrical event duration can be identified, corresponding to different interacting NF-κB complexes, so that the methodology appears to be effective also to study biological samples of considerable complexity. Ultimately, the presented data emphasize the selectivity and versatility of the functionalized nanopore device, demonstrating its applicability in bioanalytics and advanced diagnostics.

1. Introduction

Nuclear Factor-kappa B proteins (NF-κB) are the most common transcription factors in mammals. They consist in a family of related conserved proteins (Rel (c-Rel), RelA/p65, RelB, p50, and p52), able to form heterodimers and homodimers, that, upon activation by extracellular signals, are accumulated in the nucleus where they modulate target gene expression (Moynagh, 2005) (Hoffmann et al., 2006). In stationary-phase cells, NF-κB proteins are predominantly localized to the cytoplasm in an inactive form bound to the inhibitor IkB family, such as IkBα, IkBβ and Ikbε (Ghosh et al., 1998). A variety of extracellular signals, such as tumor necrosis factor alpha (TNF-α), or interleukin 1-beta (IL-1 β), can activate a signaling cascade which in turn, phosphorylating the IκB proteins, activates NF-κB. In the nucleus, the active NF-κB modifies gene expression resulting in a change of cell function. Failure of NF-κB signaling is the principal cause of several auto-immune and inflammatory disorders (Jeru et al., 2008; McDermott and Aksentijevich, 2002; Handel et al., 1995; Sweeney and Firestein, 2004; Sawada et al., 2007; Klampfer, 2011) and the relationship between NF-κB activation and oncogenesis has been supported (Pikarsky et al., 2004; Abdullah et al., 2009; Aggarwal et al., 2004; Brandi et al., 2008; Cilloni et al., 2007; Galardi et al., 2011; Puvvada et al., 2010) due to its capacity to control a large number of genes that regulate apoptosis, cell proliferation, differentiation, angiogenesis and tumor migration, especially as a consequence of chronic inflammation. For these reasons the ability to detect such proteins is a primary goal for prognostic applications.

In this study we propose to use the solid-state nanopore technology to specifically detect NF-κB proteins starting with minute amounts of biological material.

It has been demonstrated that nanopore devices are powerful tools for the sensing and the analysis of single biomolecules (Stoloff and Wanunu, 2013). Starting from the study of DNA chains (Kasianowicz et al., 1996), the application of nanopore sensors has widely grown in the last decade, thanks to the development of several strategies for improving their detection capabilities. However, the use of nanopores to sense and identify proteins and protein-DNA complexes is still challenging (Howorka and Siwy, 2012; Mahmood et al., 2014; Wei et al., 2012). In fact, proteins have a globular conformation and their detection is difficult due to the quite short translocation time through the nanopore with respect

* Corresponding author.

http://dx.doi.org/10.1016/j.bios.2014.08.081
0956-5663/

to long events produced by the passage of polynucleotides, such as DNA, that, having a linear conformation, can be schematized as long rods. However, the study of protein translocation is of fundamental importance both in basic science and diagnosis, and nanopore technology offers an unique platform for the study of protein′s shape, folding state, kinetics, charge and structure.

In the typical configuration, the nanopore is the unique path for the conduction between two reservoirs filled with an ionic solution, so that the sensing device is based on the measurement of changes in its electrical behavior: transient ionic current jumps are usually associated to biomolecule translocation, instead, more stable conductance changes are related to modification of the pore surface properties (Howorka and Siwy, 2009; Guo et al., 2011, 2012). In this second case, target biomolecules do not simply pass through the nanopore but, on the contrary, they interact with the nanopore itself. Several chemical procedures have been proposed and applied to modify and activate the pore surface and make it selective to specific target molecules dispersed in solution (Hou et al., 2011).

In this context, we have developed and characterized a chemical functionalization procedure able to both resize and activate the pore (Mussi et al., 2012). Such functionalized nanopore have been efficiently used to obtain a selective biosensor able to detect the interaction between complementary oligonucleotides (Mussi et al., 2010a, 2010b), i.e. to distinguish between oligonucleotides depending on their affinity to the functionalization.

Here we demonstrate that the functionalization procedure can be adapted and optimized to realize a single molecule sensing device that is able to recognize the recombinant p50 protein, a member of the NF-κB family. The goal is obtained by using, as probe molecule, a dsLNA containing the consensus sequence for NF-κB (see SI for NF-κB conventional signaling pathway) which is able to link the p50/p50 homodimer.

The binding between probe and target molecules has been revealed as a characteristic structuring of the current trace into well-defined levels, these current fluctuations being not present in all control experiments performed with a non-interacting sample (BSA protein) and a non-functionalized nanopore device.

Furthermore, a nuclear extract, obtained from TNF-α treated HeLa cells, was used as biological sample to perform NF-κB detection by the functionalized nanopore. Again, several current levels appear demonstrating that the device is able to identify the specific target even in samples of considerable complexity. Interestingly, in this case three main peaks can be found in the event duration distribution which might correspond to three main interacting NF-κB complexes, in agreement with previous studies (Menotta et al., 2011).

Next sections separately describe the experiments for the detection of pure p50 proteins and of the biological sample obtained by the nuclear extract. Even if the specific linkage between the probe–target interaction dynamics and the appearing current fluctuations is not completely clear and remains a complicated issue out of the scope of this paper, the presented data unambiguously demonstrate that the functionalized nanopore is a powerful and versatile platform for the selective and sensitive electrical detection of biomolecules, and represents a fast and low cost alternative to standard methods that generally require labeling and elaborate preparation of the biological sample.

2. Material and methods

2.1. Materials

The probe molecule is a double-stranded Locked Nucleic Acid (dsLNA) which is a decoy oligodeoxynucleotide (ODN). The utilized decoy contains the consensus sequence for NF-κB 5′-*TA* AGA GGG AAA TTC CGG GAA ATT CCT AC *AT*-3′. The underlined nucleotides include LNA and the sense strand of the ODN is amino-modified by a C6 bridge. Both the strands were purchased from Sigma-Proligo. The forward and reverse complements were hybridized in water to obtain 100 μM stock solution. Annealing was performed in a thermocycler with the following temperature progression: 5 min at 100 °C, followed by a temperature reduction to 37 °C over 60 min and from 37 °C to 4 °C in 30 min. The atomic mass of the p50/p50 homodimer is 100 kda.

The advantage of LNA usage is its stability in biological environment. In fact, contrary to unmodified DNA molecules, LNA molecules are not subjected to rapid degradation (due to the action of 3′-exonucleases or endonuclease attack) allowing to extend the analysis duration and to operate in a non DNAse free environment.

Two target samples are used:

P50 sample: for Figs. 2, 4 and 5 the target is the recombinant NF-κB subunit, p50 (Diatheva). p50 was preincubated with 0.2 mg/ml double-stranded non-specific DNA competitor poly(dI·dC) (Amersham Pharmacia Biotech, Piscataway, NJ) for 10 min in 14.3 μl of DBA, in ice. After the preincubation, the samples were diluted in DBA to a working solution of 300 μl (the final concentration of p50 was 0.66 ng/μl).

HeLa sample: for Fig. 6, the target biological sample containing NF-κB was prepared as follows: cervical cancer cell lines HeLa (HPV18) were obtained from the American Type Culture Collection (ATCC, Rockville, MD). Cells were cultured in Eagle′s Minimum Essential Medium (EMEM), purchased from Cambrex Bioscience Verviers, Belgium, supplemented with 10% fetal bovine serum (heat inactivated for 30 min at 56 °C), 2 mM glutamine, 100 μg/ml streptomycin and 100 U/ml penicillin. Cells were incubated at 37 °C in a 5% CO_2 atmosphere. To induce NF-κB activation, HeLa cells were stimulated by 10 ng/ml tumor necrosis factor-α (TNF-α) (Boehringer Mannheim Biochemia, Mannheim, Germany) for 30 min. After stimulation, cells were washed and harvested with cold phosphate-buffered saline. Nuclear proteins were obtained by low salt/detergent cell lysis followed by high salt extraction of nuclear proteins as previously described (Crinelli et al., 2002). The final working concentration of the whole protein extract was 3.3 ng/ml.

2.2. Nanopore fabrication

The SiN membrane was obtained by depositing a thin (20 nm or 50 nm thick) silicon nitride (SiN) film on a 300 μm thick Si substrate, and anisotropically etching the Si side of the chip to expose a squared area $80 \times 80\ \mu m^2$ squared area.

Nanopores are fabricated on the SiN membrane by ion beam milling using a CrossBeam® model 1540XB Zeiss workstation. The pore drilling is made by exposing the membrane for 1 s to a resting and focused ion beam of 2 pA.

2.3. Nanopore functionalization

The functionalization procedure can be divided into 3 steps.

Initially, an oxygen plasma treatment (60 s, 30 W) allows to clean any organic contamination and produce hydroxyl groups on the SiN surface. The entire membrane is then activated with 3-aminopropyltriethoxysilane in vapor phase for 5 min (P=30 kPa).

Then, the SiN chip is treated with 1.4-phenylene diisothiocyanate cross-linker (0.5% $P=V$ in dimethyl sulfoxide) for 1 h, followed by two washes in dimethyl sulfoxide and two washes in double-distilled water.

The final step is a 1 h treatment with dsLNA (20 nM in Hepes), followed by two washes in Tris Borate Edta buffer (TE) and ETOH 70%.

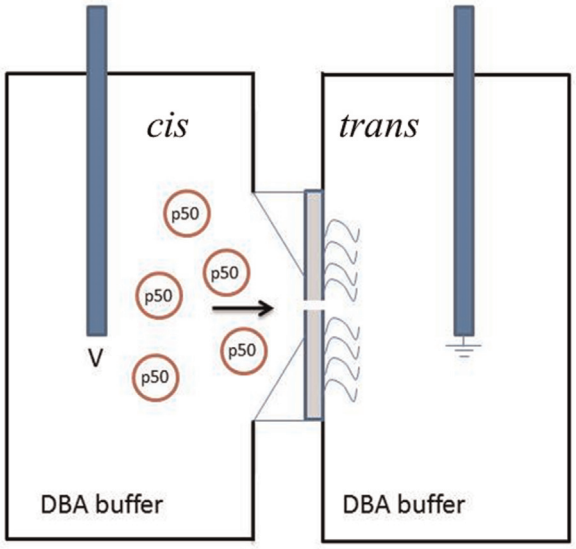

Fig. 1. Experimental setup. The functionalized nanopore is mounted between two reservoirs filled with a DNA Binding Buffer (DBA). p50 proteins are added in a reservoir and driven by the electric field through the nanopore.

2.4. Electrical sensing experiments

The experimental setup is shown in Fig. 1. The experiments are performed by inserting the SiN nanopored chip in a plexiglass chamber beween two reservoires. The system is filled with DBA solution (DNA Binding Buffer, 20 mM HEPES-KOH, pH 7.9, 0.1 M KCl, 5% v/v glycerol, 0.2 mM EGTA, 0.2 mM EDTA and 1 mM dithiothreitol) and two Ag/AgCl electrodes are inserted in the fluidic chamber. A patch-clamp amplifier (Axopatch 200B, Axon Instruments, 200 kHz sampling rate, low-pass four-pole Bessel filter set at 2 kHz) collects the ionic current which flows through the nanopore and allows to measure the nanopore conductance. A double faraday cage and an anti-vibration table are used to reduce the electrical and mechanical noises.

Target molecules are inserted in one of the two reservoirs of the fluidic chamber and are forced to migrate towards the nanopore by means of the electric field.

3. Results and discussion

3.1. P50 detection

The first set of experiments were carried out by inserting in the fluidic chamber a nanopore, drilled on a 20 nm thick SiN membrane and functionalized with dsLNA.

Fig. 2a shows a typical current trace recorded when a difference of potential (d.d.p.) of – 400 mV is applied and the chamber is filled with DBA buffer alone. The current/voltage curve (Fig. 2a) is slightly rectified due to the presence of the functionalization layer on the nanopore surface that produces geometrical and electrical asymmetries along the structure. The overall electrical resistance obtained by means of a fit of the linear region of the curve is $R = (420 \pm 20)$ MΩ. Approximating the nanopore as a cylindrical channel with a length equal to 20 nm (SiN membrane thickness), the electrical resistance can be used to calculate the "effective diameter" of the pore, d_{eff} (Mussi et al., 2010a, 2010b). Considering that the conductivity of the DBA solution is about 13 mS/cm, the obtained d_{eff} is about 8 nm. Even if this approximation does not take into account the real shape of the nanopore, the presence of

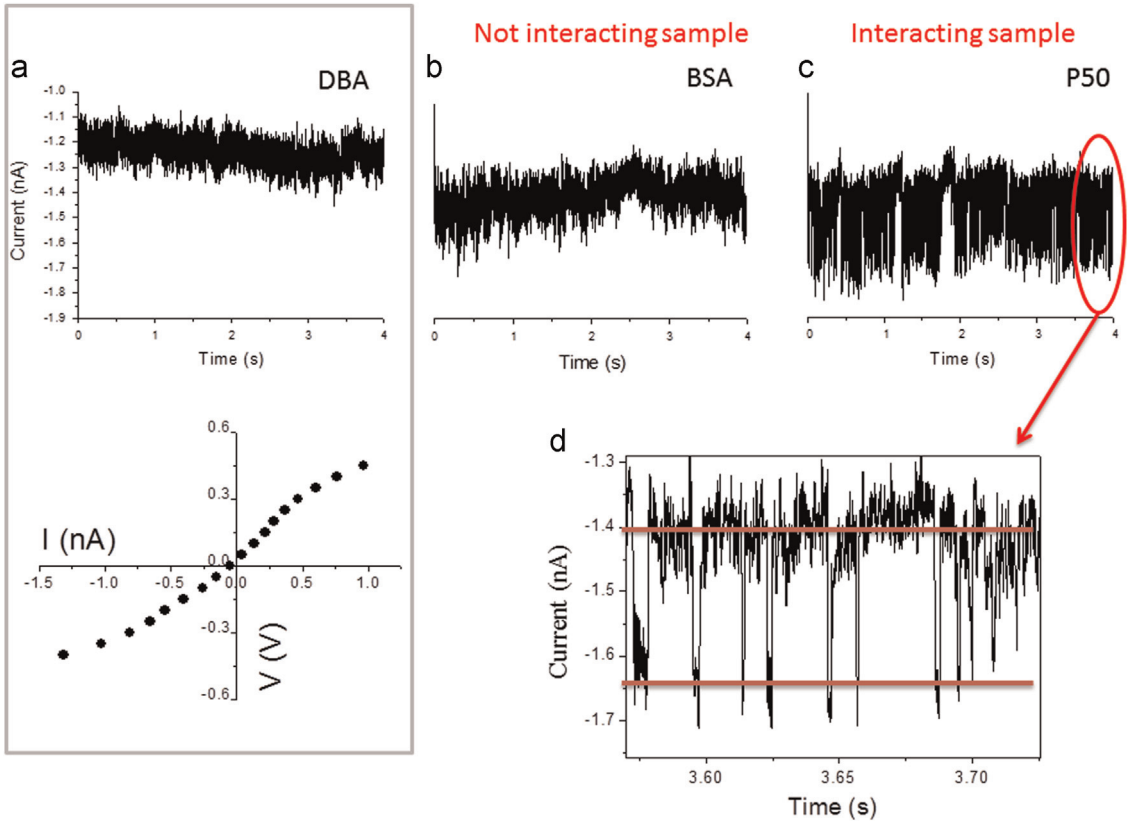

Fig. 2. p50 detection experiment. (a) Typical current trace recorded at −400 mV and current/voltage curve measured when the fluidic cell is filled with DBA buffer alone. Typical current trace recorded at −400 mV (b) after the insertion of BSA proteins in the fluidic cell as a not-interacting target; (c) after the insertion of p50 proteins in the fluidic cell as an interacting target. (d) Magnification of the current trace reported in Fig. 2c.

the functionalization layer and the effect of the surface charge on the measured conductance, the effective diameter gives us a reasonable estimate of the dimension of the functionalized pore, which is very close to the steric dimension of the target proteins.

A test experiment has been then performed by inserting BSA proteins in the fluidic cell as a not-interacting target, to verify the specificity of the detection mechanism. In this case, as shown in Fig. 2b, the current trace is noisier with respect to that obtained with DBA solution alone and the mean current value increases of about 200 pA. Actually, this behavior is observed every time a charged target sample is inserted in one of the reservoirs, and can be ascribed to the establishment of asymmetric buffer conditions between the two sides of the nanopore. However, the recorded traces do not exhibit any specific fluctuation imputable to protein translocation or probe–target interaction occurring on long time scale, even after 15 min of recordings. In fact, BSA protein translocation is unlikely to occur in such a small nanopore and, in case, the passage is expected to be so fast (Larkin et al., 2014; Storm et al., 2005) that the associated signal is filtered out by the 2 kHz low-pass filter applied before sampling. Thus, the data of Fig. 2b clearly demonstrate the substantial absence of un-specific interaction between the chemically modified nanopore and the target molecules.

Afterwards, target p50 molecules are diluted in the DBA buffer, inserted into the fluidic cell, and driven through the functionalized nanopore by the electric field. Fig. 2c shows a current trace recorded at −400 mV when p50 is present inside the fluidic cell. In this case, several fluctuations appear, associated to distinguishable current levels. A magnification of the current trace of Fig. 2c is shown in Fig. 2d which allows to better visualize the presence of well-separated levels.

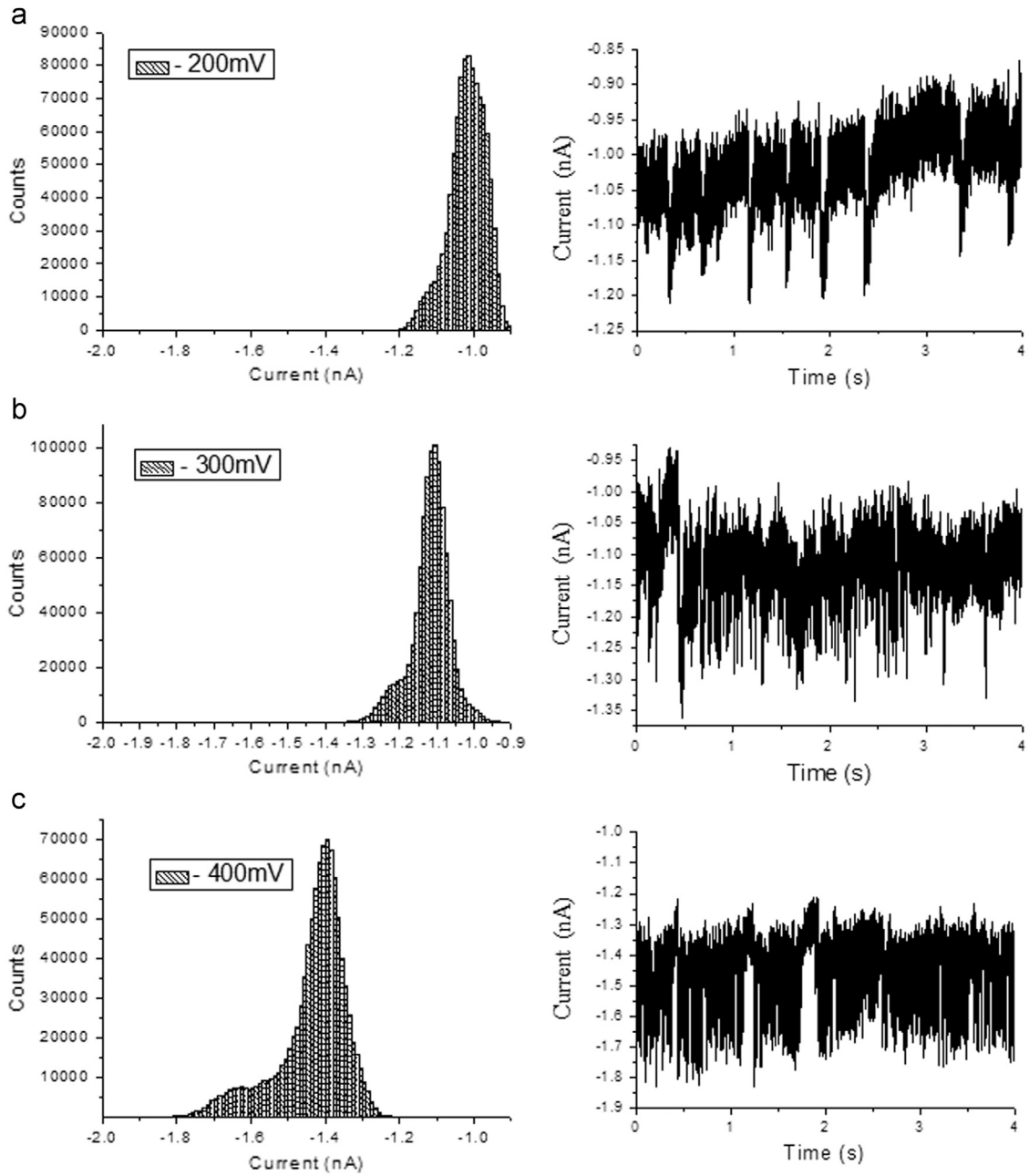

Fig. 3. Current level histograms. Current histograms and examples of current traces recorded at (a) −200 mV, (b) −300 mV and (c) −400 mV. Two peaks appear at each applied voltage corresponding to two conductance levels of the nanopore associated to the formation of a probe–target complex.

To analyze the data consisting of several traces collected for each voltage bias, we computed the all-point current histograms at −200 mV (Fig. 3a), −300 mV (Fig. 3b) and −400 mV (Fig. 3c).

Two peaks appear at each applied voltage corresponding to two conductance levels of the nanopore associated to the formation of a probe–target complex. In fact, when p50 target proteins are inserted into the fluidic cell and driven towards the nanopore, they start to interact with the functionalization layer. The force exerted on the probe–target complex by the applied voltage can be roughly estimated by neglecting viscous forces and protein–protein interactions, and considering the electrical charge of p50 at physiological pH to be about −2e. When applying −400 mV across a 20 nm pore, the force is thus about 6 pN. This value must be compared with the binding force between NF-κB and the dsLNA probe, which ranges from 50 to 250 pN (mean value of 119 pN) (Menotta et al., 2011). Therefore, the binding force is at least one order of magnitude higher than the force due to the applied voltage, suggesting that binding events are strong enough to prevent the dislodging of the protein from the nanopore by the applied bias.

Although we do not leave out the existence of a complex dynamic of binding–unbinding poorly influenced by the electric field, we conclude that the binding between probe and target molecules is stable.

In this picture, the two peaks observed in the histograms of Fig. 3, are associated to variable conformations of the probe–target complex causing an oscillation of the trace between an "on state" with higher current, which corresponds to a partially open pore, and an "off state" with lower conductance.

By increasing the applied voltage, the mean current level increases and, as expected, the distance between the two current levels ($\Delta I = I_{open} - I_{closed}$), being proportional to the diameter of the pore and to the applied voltage, increases accordingly.

Interestingly, the occupation probability of the "off state" is higher with respect to that of the "on state", due to the presence of the electric field that pushes the p50–dsLNA complex close to the entrance of the nanopore.

The complexity of the recorded current traces does not allow to give a more complete and simple explanation of the process. However, the principal finding is evident and reproducible: current fluctuations associated to precise current levels only appear when the fluidic cell is filled with a sample specifically interacting with the functionalization layer. The result is quite similar to that obtained with different interacting biomolecules (Mussi et al., 2011), demonstrating the remarkable potentiality and versatility of the nanopore biosensor which is generally able to identify the specific interaction between probe molecules attached to the pore walls and complementary target molecules in solution.

To better understand the current behavior correlated to the interaction between proteins and the functionalized nanopore, we have performed different experiments by inserting the target sample either in the *cis* (containing the biased electrode) and in the *trans* (whose electrode is always grounded) reservoirs and changing the orientation of the SiN nanofored chip. Fig. 4 shows the four different configurations that we have tested.

The data demonstrate that the interaction between target and probe molecules is effective, giving rise to the revealed fluctuations, only when the SiN side of the membrane, i.e. the functionalized one, is placed so that the dsLNA molecules attached on the pore surface are pushed to enter inside the nanopore from the applied electric field (configuration of Fig. 4a and d). This behavior depends on the specific structure of the nanopore chip, which consists of a thin SiN membrane deposited on a Si support. In fact, the chemical modification procedure is performed by placing the chip on a petri dish on its Si side, so that all the activation steps are carried out on the SiN side, giving rise to an asymmetric

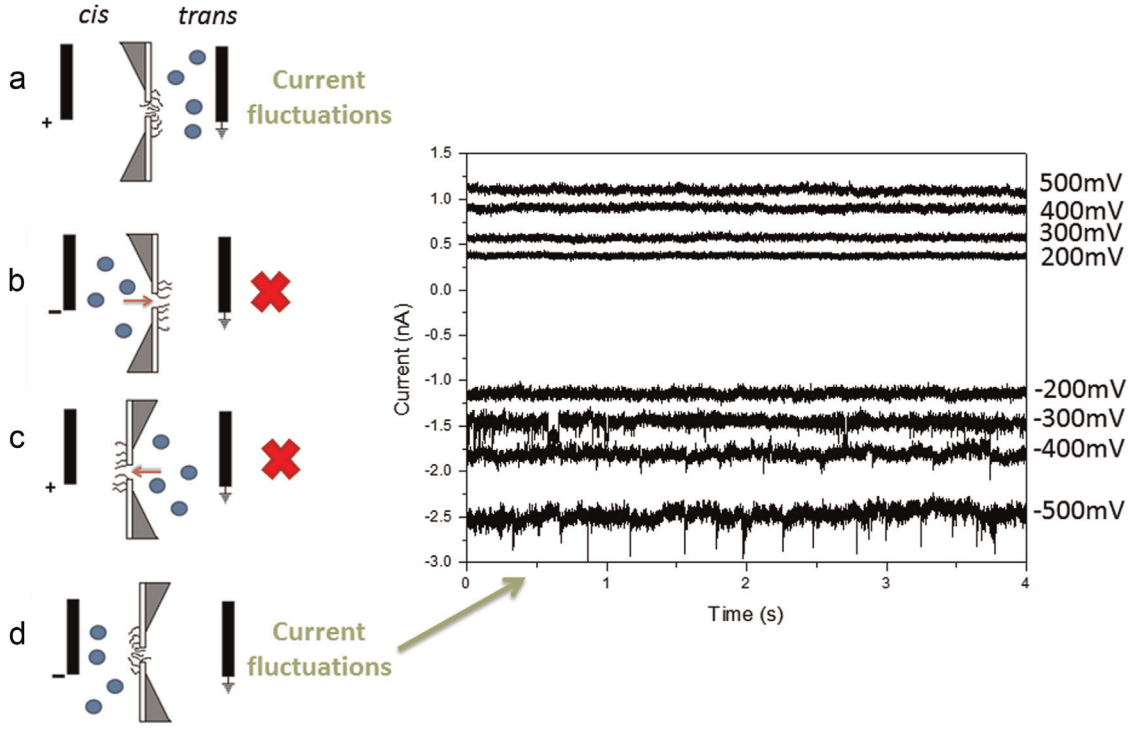

Fig. 4. Directionality of protein detection. (a)–(d) Four experimental configuration that has been tested. Sketch illustrates the behavior of dsLNA molecules attached to the nanopore surface by changing the electrode polarity and the orientation of the SiN nanopored chip. On the right, current traces recorded at different applied voltages after the insertion of the p50 sample into the fluidic cell (configuration *d*).

functionalization of the device, that also produces an asymmetric voltage/current curve, as previously underlined.

Thus, looking for example at the case of Fig. 4a, when a positive voltage is applied, to induce translocations of the target inserted in the trans reservoir, the formed probe–target complex, being negatively charged, is driven into the pore and creates the partial obstruction revealed as current fluctuations. This situation does not occur for negative bias, that are applied when the target is inserted in the *cis* reservoir (Fig. 4b).

Moreover, the interaction of p50 with all dsLNA probes attached on the entire SiN membrane causes a reduction of the actual concentration of free translocating target molecules and an energy penalty for further proteins to reach the nanopore (Wanunu et al., 2008). The presence of an electrical barrier that target molecules experience when forced to go through the nanopore is confirmed by the fact that there is a threshold voltage beyond which the detection of current fluctuations is prevented. Fig. 4 and the histogram in Fig. 3 show that at 200 mV the current fluctuations are sporadic, and below this value of applied voltage it is impossible to detect events. The presence of a threshold voltage to drive proteins into the nanopore has been observed also by Wu et al. (2014).

Control experiments have been realized with nanopores having a greater length of about 50 nm, in order to confirm the fact that the revealed current levels are not related to translocation events, hard to be seen in such thick nanopores, but rather to the formation and "toggling" of complexes of proteins stably attached to the probe dsLNA. A typical trace recorded at 500 mV is shown in Fig. 5a. Similarly to the case of pores drilled into thin membranes (20 nm thick), the current traces collected after p50 insertion into the fluidic cell are characterized by evident variations associated to the stable binding of target proteins to LNA molecules covalently attached to nanopore walls.

Further control experiments have been performed by using non-functionalized nanopores drilled on a SiN membrane 20 nm thick. The protein p50 was diluted in DBA and inserted into the fluidic cell. Fig. 5b shows a typical current trace recorded at 500 mV after the insertion of the p50 sample. In this case, no signal has been detected, demonstrating the fundamental role of the functionalization layer in the detection process. Actually, as previously underlined, protein translocations, if they occur, are too fast to be recorded in the absence of a selective interaction with the pore strongly altering the process dynamics. Furthermore, the functionalization layer not only activates the pore, making it selective to specific target molecules, but also resizes the initial diameter from 30–40 nm to a final figure of 5–10 nm, thus increasing the sensitivity of the device (Mussi et al., 2012).

The proposed device does not give quantitative information but rather an "on–off" response to the presence of the target sample. We have performed experiments with different concentration of p50 proteins (up to 2.5 ng/μl) finding that the "toggling behavior" occurs at every concentration, demonstrating that it is actually and uniquely due to the presence of the interacting sample. In this paper, we have presented data obtained with the most diluted sample between those used for the tests.

3.2. HeLa sample detection

Finally, we performed experiments with a biological sample obtained by preparing a nuclear extract from TNF-α treated HeLa cells in order to detect different members of the NF-κB family. The result is shown in Fig. 6a which reports a typical current trace recorded at 200 mV after the insertion of the biological sample. Again, the appearance of typical current fluctuations can be observed, as better visible in the magnification of Fig. 6c. These fluctuations cannot be observed if only DBA buffer is inserted in the fluidic cell with the same functionalized pore.

The all point current histogram of the trace in Fig. 6a is reported in Fig. 6b. Two principal levels can be recognized, associated to the open pore current and to the reduced current resulting from an occupied state for the pore, thus confirming the presence of the interacting molecules in the sample (that we hypothesize belonging to the NF-κB family). This experimental case is much more complicated with respect to the previous one, where p50 alone was present. In fact, more kinds of NF-κB proteins can interact with the pore with a different level of strength. Moreover, target proteins can also interact with other cellular components present in the sample modulating the binding to dsLNA and forming larger structures. For these reasons, we evaluated the dwell time distribution for the occupied level which is shown in Fig. 6d. There is a large variability in the duration of the collected events confirming that the observed current fluctuations cannot be associated to translocation processes but rather to the rich interaction dynamics of molecules inside the pore. This idea is supported by the fact that it is possible to find three principal peaks in the dwell time distribution by means of a multi-Gaussian fit. These peaks are associated with different event durations (0.59 ms, 2.1 ms, 3.4 ms) that might correspond to three main interacting NF-κB complexes. In a previous study the interaction strength between the dsLNA and captured NF-κB from HeLa cells was evaluated by force–distance spectroscopy with an atomic force microscope. It is striking and fascinating to note here that, also in that case, three main strength peaks were revealed (Menotta et al., 2011). These evidences reinforce our belief that

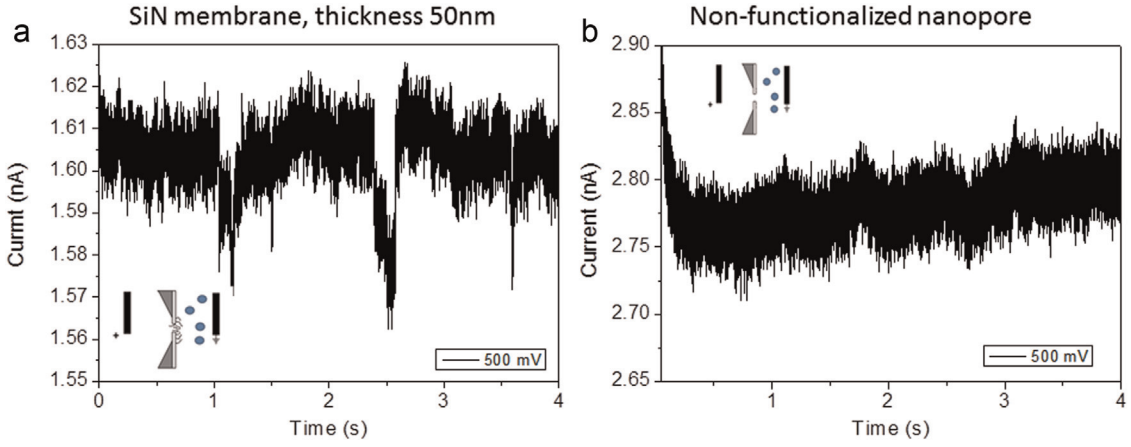

Fig. 5. Control experiments. Typical current traces recorded at 500 mV after the insertion of p50 proteins in the fluidic cell by using (a) a functionalized nanopore drilled in a 50 nm thick SiN membrane, and (b) a non-functionalized nanopore.

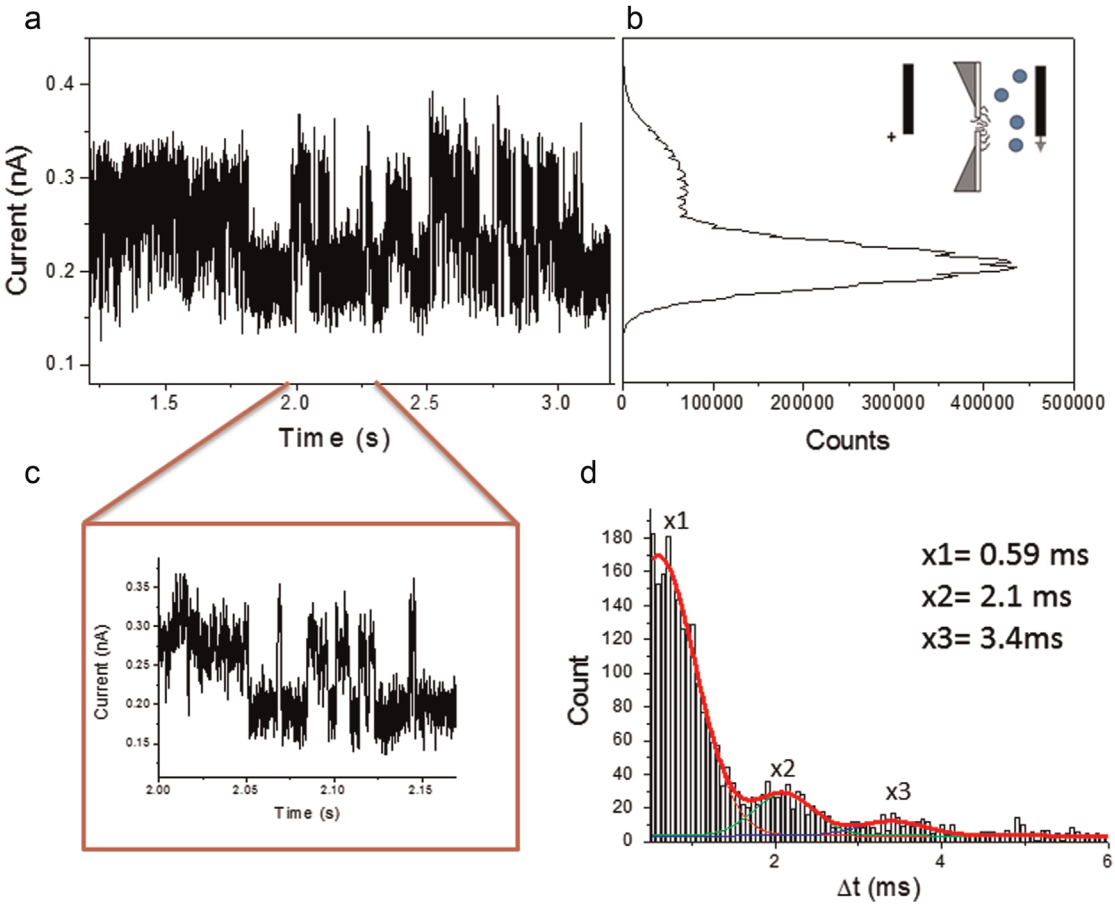

Fig. 6. HeLa detection experiment. (a) Typical current trace recorded at 200 mV after the insertion of the biological sample obtained by preparing a nuclear extract from TNF-α treated HeLa cells. (b) All point current histogram of the trace reported in (a). (c) Magnification of the trace reported in Fig. 6a. (d) Dwell time distribution for the occupied level (200 pA).

nanopore technology can be used as an effective methodology to study biological samples of considerable complexity.

4. Conclusions

In the present paper, we have shown that a simple functionalization procedure allows to activate a SiN nanopore obtaining a successful electrical biosensing device able to specifically detect biomolecules dispersed in a buffer solution. In particular, we have proven the capability of the functionalized nanopore to selectively detect NF-kB binding activity in a label-free manner. Furthermore, we have shown that the same method can be applied to directly detect NF-κB in a whole cell extract.

The recorded current fluctuations can be ascribed to a complicated toggling behavior of the complex formed by the probe molecules attached the pore surface and the target ones in solution. In fact, only in presence of a sample specifically interacting with the pore, the distribution of current values exhibits two peaks corresponding to as many "occupancy states" of the nanopore.

Given the very small amount of biological sample needed to perform the proposed sensing, this system could be coupled with standard prognostic practice in order to use NF-κB activation state as a molecular marker, and fetch nanopore technology into the clinic research.

Acknowledgments

We would like to thank Dr. Simona Valleggi for the precious contribution during the experiments, Mauro Chinappi for useful discussion, Fondazione Bruno Kessler, FBK, for the Si/SiN chip fabrication and ElbaTech S.r.l. for the microfluidic cell construction.

This work has been supported by the Italian Ministero dell' Università e della Ricerca (MIUR) with the National Projects NANO-MAX, the FIRB Project NEWTON and by the University of Genoa (Italy) Research Grant PRA 2012 (Progetti di Ricerca di Ateneo).

Appendix A. Supplementary information

Supplementary data associated with this article can be found in the online version at http://dx.doi.org/10.1016/j.bios.2014.08.081.

References

Abdullah, M., et al., 2009. Acta Med Indones 41, 70–74.
Aggarwal, B.B., 2004. Cancer Cell 6, 203–208.
Brandi, G., Pantaleo, M.A., Biasco, G., Paterini, P.J., 2008. Clin. Oncol. 26, 1388–1389.
Cilloni, D., Martinelli, G., Messa, F., Baccarani, M., Saglio, G., 2007. Haematologica 92, 1224–1229.
Crinelli, R., Bianchi, M., Gentilini, L., Magnani, M., 2002. Nucleic Acids Res. 30, 2435–2443.
Galardi, S., Mercatelli, N., Farace, M.G., Ciafrè, S.A., 2011. Nucleic Acids Res. 39, 3892–3902.
Ghosh, S., May, M.J., Kopp, E.B., 1998. Annu. Rev. Immunol. 16, 225–260.
Guo, Z., Wang, J., Wang, E., 2012. Talanta 89, 253–257.

Guo, Z., Wang, J., Ren, J., Wnag, E., 2011. Nanoscale 3, 3767.
Handel, M.L., Mcmorrow, L.B., Gravallese, E.M., 1995. Arthritis Rheum. 38, 1762–1770.
Hoffmann, A., Natoli, G., Ghosh, G., 2006. Oncogene 25, 6706–6716.
Hou, X., Guo, W., Jiang, L., 2011. Chem. Soc. Rev. 40, 2385–2401.
Howorka, S., Siwy, Z.S., 2012. Nat. Biotechnol. 30, 506.
Howorka, S., Siwy, Z., 2009. Chem. Soc. Rev. 38, 2360–2384.
Jeru, I., et al., 2008. Proc. Natl. Acad. Sci. 105, 1614–1619.
Kasianowicz, J.J., Brandin, E., Branton, D., Deamer, D.W., 1996. Proc. Natl. Acad. Sci. 93, 13770–13773.
Klampfer, L., 2011. Curr. Cancer Drug Targets 11, 451.
Larkin, J., Henley, R.Y., Muthukumar, M., Rosenstein, J.K., Wanunu, M., 2014. Biophys. J. 106, 696–704.
Mahmood, M.A.I., Ali, W., Adnan, A., Iqbal, S.M.J., 2014. Phys. Chem. B (Just Accepted Manuscript doi:10.1021/jp411820w).
McDermott, M.F., Aksentijevich, I., 2002. Curr. Opin. Allergy Clin. Immunol. 2, 511–516.
Menotta, M., et al., 2011. Biosens. Bioelectron. 28, 158–165.
Mussi, V., Fanzio, P., Firpo, G., Repetto, L., Valbusa, U., 2012. Nanotechnology 23, 435301.
Moynagh, P.N., 2005. J. Cell Sci. 118, 4589–4592.
Mussi, V., et al., 2010a. J. Phys. Condens. Matter 22, 454104.
Mussi, V., et al., 2010b. Nanotechnology 21, 145102.
Mussi, V., et al., 2011. Biosens. Bioelectron. 29, 125–131.
Pikarsky, E., et al., 2004. Nature 431, 461–466.
Puvvada, S.D., et al., 2010. Oncology 78, 181–188.
Sawada, H., et al., 2007. CHEST J 132, 1265–1274.
Stoloff, D.H., Wanunu, M., 2013. Curr. Opin. Biotechnol. 24, 699–704.
Sweeney, S.E., Firestein, G.S., 2004. Curr. Opin. Rheumatol. 16, 231–237.
Storm, A.J., et al., 2005. Nano Lett. 5, 1193–1197.
Wanunu, M., Sutin, J., McNally, B., Chow, A., Meller, A., 2008. Biophys. J. 95, 4716–4725.
Wei, R., Gatterdam, V., Wieneke, R., Tampé, R., Rant, U., 2012. Nat. Nanotechnol. 7, 257–263.
Wu, L., et al., 2014. Nanoscale Res. Lett. 9, 1–10.